Very High-Pressure Sprays of Gasoline from a GDI Multi-hole Injector

Alessandro Montanaro*[1], Luigi Allocca[1], Giovanni Meccariello[1], Angelo De Vita[2]
[1]Istituto Motori, National Research Council, Napoli, Italy
[2]Università degli Studi dell'Aquila, L'Aquila, Italy
*Corresponding author: a.montanaro@im.cnr.it

Abstract
In GDI engines, the atomization process of the fuel is known to play a key role in affecting mixture formation, combustion efficiency and soot emissions. Multi-hole injectors have been widely used in GDI engines due to their flexibility in controlling jet targeting and fuel distribution. Therefore, successful implementation of GDI technology needs precise knowledge of the fuel injection process and proper understanding of spray characteristics under engine relevant conditions. The injection system needs to improve the spray characteristics in terms of a better fuel atomization in shortest possible penetration length, refined droplet sizes and better droplet size distribution to enhance a combustion system efficiency. In this context, the increasing of the fuel injection pressure seems to play a key role.
This paper reports the results of an investigation on the behavior of gasoline injected at very high-pressure by a GDI injector in a combustion vessel filled with gas (N_2) at diverse ambient pressures and temperatures. The injector was a ten-hole nozzle, solenoid-actuated, 0.10 mm in diameter while the injection pressures varied up to 70 MPa, the gas density from 0.2 to 11.50 kg/m^3 and ambient temperature from room to 200°C. The investigation was carried out by optical techniques using a high-speed C-Mos camera and permitting to depict the propagation of the liquid fluid through Mie-scattering and the global (liquid + vapor phases) by shadowgraph technique. The influences of ambient and injection conditions were of particular interest providing fundamental physics insight regarding fuel penetration and vaporization

Keywords
High injection pressure, liquid-vapor phase, flash boiling.

Introduction
In the modern GDI system for gasoline engines, the optimization of the fuel injection process is essential to prepare an air-fuel mixture capable to promote an efficient combustion and reduce both fuel consumption and pollutant emissions. In particular, the fuel injector will be a key component and features such as advanced nozzle design and manufacturing process, high-pressure fuel system, controlled injection rate, multiple injections in conjunction with precise minimum-injected quantities, will be pursued to improve the fuel economy and reduce pollutant emissions. This renders the injector technology a primary enabler for advancing the GDI engine combustion characteristics. In this context, the increasing of the fuel injection pressure is believed a key feature for achieving these targets [1]. Moreover, it is considered a good way for particle number (PN) reduction due to improved spray atomization, faster evaporation, and better mixture formation [2, 3]. More, previous scientific research found that the high injection pressure produced a strong effect on the PM for both number and mass and that this method represents a way to reduce the emission of the soot [4]. The tendency was acquired from the diesel environment but the reduced displacement and the downsizing vocation of the spark ignition (SI) engines produces in a drawback of fuel impacting on the piston head and cylinder wall with film deposition, lower vaporization, and production at the exhaust of unburned hydrocarbons and soot. Flash boiling phenomena is considered an other relevant way to produce an optimal fuel spray with advantages in generating finer droplets, enhancing fuel/air mixture, improving the combustion, and reducing PN emissions [5-9]. Flash boiling, which features a two-phase flow that constantly generates vapor bubbles inside the liquid spray is ideal to achieve fast evaporation and combustion inside direct-injection (DI) gasoline engines. It occurs when liquid fuel is injected into an ambient environment below its saturation pressure. Many studies were implemented to understand the features and mechanisms of flash boiling sprays under conventional injection pressures (lower than 20.0 MPa) but few studies have been done to investigate how the spray structure varies at very-high pressure of the injections.
The focus of this study was to quantify the effects of fuel injection at high pressure on gasoline spray development for a wide range of ambient conditions, including sub-atmospheric ones. Liquid and vapor fuel phases were investigated under evaporative and non-evaporative conditions mainly to study the effects of very-high injection pressures (up to 70.0 MPa) on spray morphology. Commercial gasoline was injected by an adapted GDI injector in

a constant volume vessel (CVC) filled with gas (N_2) at diverse pressures and temperatures. The injector was a ten-hole nozzle, solenoid-actuated, 0.10 mm in diameter. The injection pressures ranged from 40.0 to 70.0 MPa, the gas density from 1.12 to 11.50 kg/m^3 and the ambient temperature from room to 200°C. Investigation by optical techniques, using a high-speed C-Mos camera, permitted to depict the liquid propagation through Mie-scattering, for the liquid, and the shadowgraph for the global (liquid + vapor phase).

Material and methods

A high-pressure GDI injector, mounted on the top of a constant volume chamber, injected commercial gasoline (density 0.72 kg/l @ 20°C) with initial and final boiling points 35°C and 200°C, respectively, at atmospheric pressure. The nozzle has ten identical holes with diameter (d_0) of 100 µm and L/d=7, having a static flow of 10.55 g/s @10.0 MPa. The fuel is supplied through a rail, heated by an electrical resistance and controlled in temperature by a J-type thermocouple. A governor achieved the nozzle and fuel temperature managements via a remote computer. A cooling cup surrounding the injector mount was used to realize the injector temperature. Both the injector (T_i) and the fuel temperature (T_{fuel}) were kept constant at 20°C for the conventional conditions while at 90°C for the flashing ones. The ambient temperature (T_{amb}) inside the vessel ranged between room and 200°C. An air-driven pneumatic pump was used to set the injection pressure collected by a transducer just before the injector entrance. The tests were carried out at the injection pressures (p_{inj}) of 40.0, 55.0, and 70.0 MPa and for diverse ambient densities (ρ_g) ranged from 0.2 to 11.5 kg/m^3. The chamber was purged and filled with nitrogen, and its ambient pressure (p_a) was regulated by a vacuum pump, for sub-atmospheric values, and by a high-pressure nitrogen charging for the other. The injector driving parameters were adjusted as a function of fuel pressure and were generated by a home-made electronic control unit, keeping constant at 1.0 ms the energizing time (t_{inj}). The spray morphology was investigated by two optical techniques, shadowgraph and Mie-scattering, acquiring the images along the same line-of-sight. This optical setup was arranged to visualize the liquid phase from Mie scattering images while the corresponding shadowgraph were employed to underline the vapor phase. A pulsed LED (Omicron LEDMOD V2 - 470nm / 450mW) was used as the shadowgraph light source while a high-intensity flash, synchronized with the injection event, provided the illumination for Mie-scattering. The spray images were collected by a high-speed C-Mos camera (Photron FASTCAM SA4), at a rate of 16,000 frames per second (fps) with an image window of 512x448 pixels. The camera was equipped with a 90 mm objective, f 1:2.8, resulting the spatial resolution 5.90 pixel/mm. The images acquired in the different operating conditions were analyzed by means of a post-processing software developed in C# environment. Single frames were extracted from the high speed videos and binarized in order to locate the spray boundary, for both liquid and vapor phases. The methodology to assess the sensitivity of the threshold value was described in previous studies [10]. The resulting spray images were then processed to compute the main macroscopic features of the spray, according to SAEJ2715 rule [11]. More details on optical setup as well as the adopted images processing procedure are reported in [12].

Results and discussion

The effects of the injection pressure on liquid spray morphology are reported in Figure 1 for ambient densities of 1.12 (top) and 11.5 kg/m^3 (bottom), and injection pressures of 40.0 (left), 55.0 (middle), and 70.0 MPa (right). The liquid structure is depicted by Mie scattering images at room temperature when the spray is completely developed, t_{inj}: 625 µs @ ρ_g: 1.12 kg/m^3 and t_{inj}: 1000 µs @ ρ_g 11.5 kg/m^3.

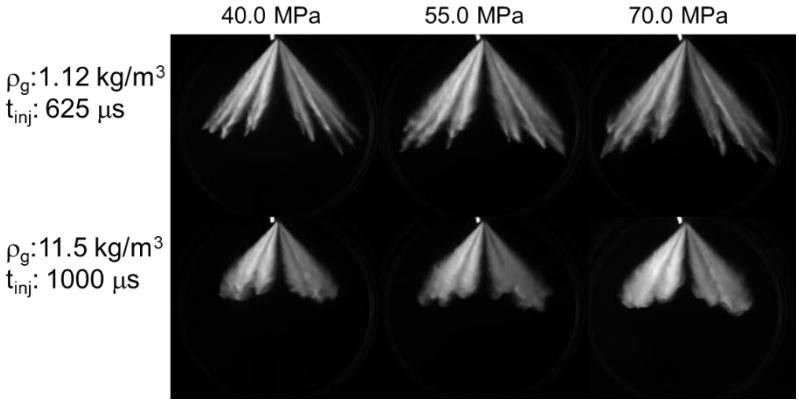

Figure 1. Liquid spray images at different injection pressures and ambient densities; T_{amb}:20°C.

The total amount of injected fuel increases at increasing of the injection pressure, keeping constant the solenoid energizing time. The shapes of the sprays appear structured into two lobes outlining the division of five jets per lobe with respect to the C-Mos camera line of sight. At atmospheric conditions of the gas (top) the evolution of the single plumes are still visible while, at the increasing of the gas density (bottom) the jets become undistinguishable. An

increase of the umbrella cone angle is registered and two main compact lobes appear. The images show visible growth of light scattering by the spray plumes with increasing of the injection pressure, as consequence of the greater amount of the fuel injected. At atmospheric condition, the spray images show insignificant effects of the system pressure on the spray penetration, whereas the spray plume width becomes wider when the injection pressure increases from 40 MPa to 70.0 MPa. Vice versa, just a slight tendency to increase the fuel penetration with growing the injection pressure can be noticed for the condition with 11.5 kg/m^3 as gas density (simulating injection conditions during the compression stroke). As a confirmation, the liquid penetration lengths of the spray in Figure 2 show differences of the fuel tip development versus time as function of the diverse injection pressures and ambient densities. The spray penetration length is defined here as the maximum distance between the nozzle exit and farthest point of the spray tip along the spray axis. Each data point is an average of 5 injection events, and the error bars are the standard deviation of the data.

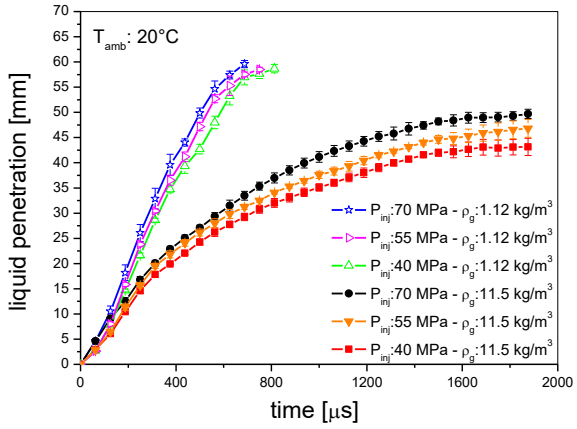

Figure 2. Liquid spray penetration at different injection pressures and ambient densities.

The profiles indicate a stronger sensitivity of the spray development to chamber pressure in comparison with fuel injection pressure. In fact, the curves gather three by three because the ambient density is the main controlling parameter. The similarity in penetration distance at early times indicates the different chamber pressures as well as the injection pressures cause similar effects on initial spray development. Later, after the break-up time, there is a strong chamber pressure dependence, which is consistent with expectations for spray development at later times when fluid mixing and entrainment dominate, while slight variation with the injection pressure is registered. These trends differ from the typical spray evolution under conventional injection pressure values (lower than 20.0 MPa) where the increasing of the injection pressure generates a significant increase of the spray penetration. The effect of the highest fuel momentum as consequence of the greatest injection pressures looks to be balanced from the effect of the strongest fuel atomization that produces the reduction of the droplet size and, therefore, a spray development braking.

The influence of the ambient temperature on the spray evolution at the gas density of 5.7 kg/m^3 is illustrated in Figure 3 through spray evolution at 200°C as ambient temperature and 55.0 MPa as injection pressure. Mie scattering (top) for the liquid and shadowgraph (bottom) spray images for liquid and vapor phases are reported at different time from the start of injection (SOI). The consequences of the temperature increase on the liquid part of the spray were well emphasized by the images collected by the Mie-scattering technique giving an immediate evidence of the vaporizing process. A strong reduction along of both the axial and the radial direction was registered because of the vaporization that mainly affects the jets periphery, where stronger atomized particles are present. The shadowgraph pictures clearly show a dense liquid core (dark part), liquid portion, surrounded by an area including ligaments, finely atomized droplets, and vapor phase.

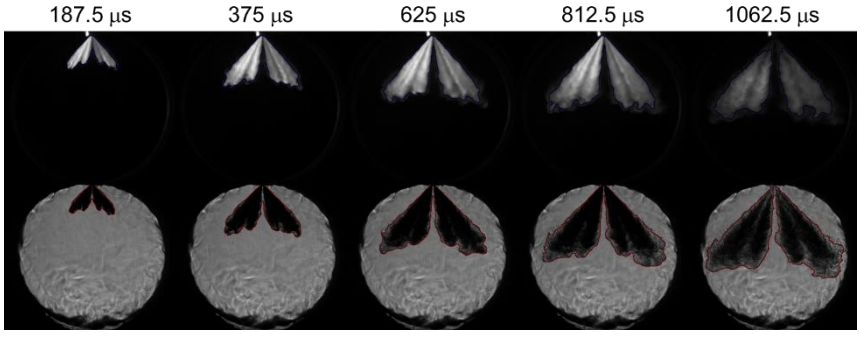

Figure 3. Mie scattering (top) and shadowgraph (bottom) spray evolution; p$_{inj}$: 55.0 MPa, ρ$_g$: 5.7 kg/m^3, and T$_{amb}$: 200°C

The corresponding spray penetration profiles versus time are reported in Figure 4(a). Red line (signed as global) reports the results from the shadowgraph images permitting to evaluate the development of both liquid and vapor phase while the liquid profiles are obtained from the scattering images and are depicted by black line. Under evaporative conditions, the spray forms and develops as follows: at the beginning, the liquid phase atomizes and progresses. In meanwhile, enough heated gas is entrained to warm and vaporize the fuel. Then, the liquid penetration slows down while the vapor phase still penetrates. The liquid spray became skinny and the penetration reduces because of the evaporation process. The short error bars per all along the spray evolution confirm the stability of the spray shape repetitions. Similar behavior was carried out from the spray at injection pressures of 40.0 and 70.0 MPa, not reported here. Figure 4(b) depicts the ambient temperature effects on spray penetration for liquid phase at p_{inj}: 70.0 MPa and ρ_g: 5.7 kg/m^3. Basically, the general trend showed a well-scaled penetrations vs. ambient temperatures with a strong inverse effect. Under non-evaporative conditions, the plumes are constituted essentially of liquid part, the jets are bulky and longest penetrations are reached (20°C). At early stages a slight diversification appears with more penetrating fluid at the lowest temperatures of 20 and 100°C and a reduced penetration for 200°C one. Later, the penetration begin to differ each other at increasing of the ambient temperature because of the evaporation process.

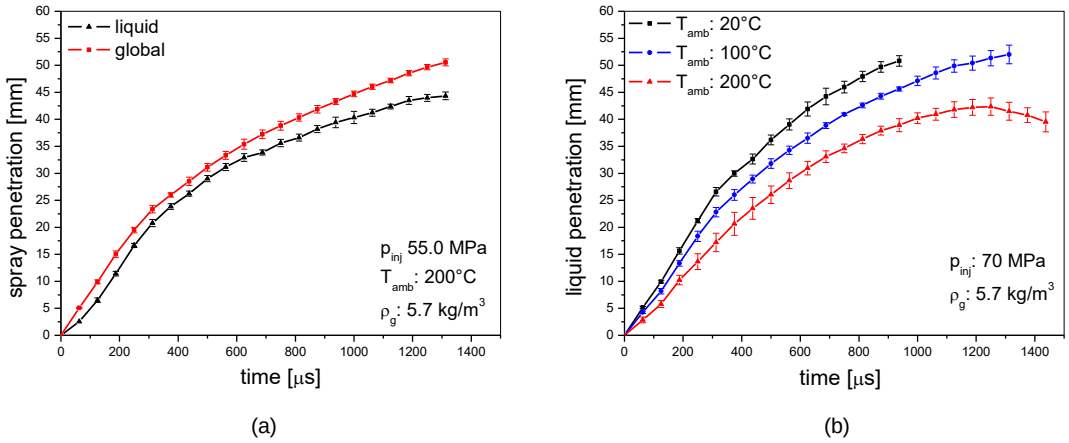

Figure 4. (a) Liquid and global spray penetration profiles at 200°C and 5.7 kg/m^3 as ambient temperature and density, respectively. (b) Effect of different ambient temperature on liquid spray penetration at gas density of 5.7 kg/m^3 and p_{inj}:70 MPa.

In the last section of the work, we will discuss on flash boiling conditions under higher injection pressure. As known, the increasing of the fuel temperature combined with the reduction of the ambient pressure is a common way to increase the fuel superheat degree and thereby increase the spray flash-boiling effect. For multi-hole fuel injectors, a high level of flash boiling causes the plumes to merge into a single plume, usually better-known as “spray collapse”. As consequence of this phenomenon, a thinner and longer spray is generally generated [10]. It would increase the possibility of fuel-wall impingement in engines due to its longer spray penetration, which might result in a significantly increased amount of fuel adhered on the wall of the combustion chamber, and consequently cause the deposit, soot, and super-knock [13]. The increasing of the injection pressure can be considered an option to suppress the plume-to-plume interaction of flash-boiling spray. The experimental results of the injection pressure impact were summarized in Figure 5, where contours of the liquid and vapor phases of the spray, superimposed to the shadowgraph images are shown at the fixed time of 625 μs from SOI. The inner (blue) contours were derived from the Mie scattering images and represent the liquid phase. The outer (red) contours were derived from the shadowgraph images and include the liquid core and vapor phase. The overlaying of the liquid phase contour onto the shadowgraph image allows the determination of the line-of-sight phase boundary.

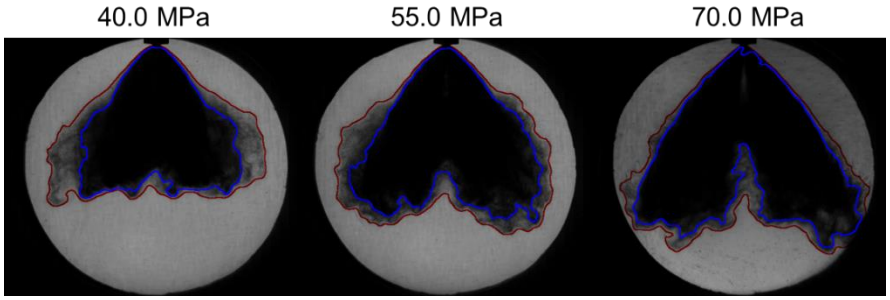

Figure 5. Shadowgraph spray images under flashing conditions, effect of injection pressure

Figure 5 shows that the evaporation was enhanced along the entire spray edge. This is due to the air entrainment on the boundary of the spray that enhances the heat transfer of the droplet with the ambient air, and promotes the evaporation along the perimeter of the spray. In this part of investigation, both the fuel (T_{fuel}) and injector (T_i) temperature were fixed to 90°C and the ambient pressure at 0.02 MPa realizing an ambient density of 0.23 kg/m^3 being the ambient temperature constant at room value. From the spray images in Figure 5, it appears clear how the elevation of injection pressure reduced the plume-to-plume interaction under the same fuel temperature and ambient pressure. At the lowest injection pressure (40.0 MPa), the spray plumes become fully collapsed to form a single body. Large vapor vortexes are visible at the bottom part of the spray and the individual plumes are no more identifiable. At increasing of the injection pressure (55.0 MPa), the characteristic spray collapse shape looks less evident: the vapor vortexes disappear, the spray cone angle increases and the global spray begins to separate into two main lobes. Finally, at further increasing of the injection pressure (70.0 MPa), the spray appears almost completely separated in two with a gap in the middle and the collapsed structure is not more evident. As a consequence of the flash boiling phenomenon, the collapse of the spray is usually interpreted as that the adjacent plumes that are expanded by the flash boiling and are connected in a ring shape, forming a closed region in the center of the spray. Hence, no ambient gas can be transferred from the outside to the closed central region, which leads to pressure reduction in the central region and, further, all plumes deviates towards the central axis. This characteristic outcome of the spray, when flash boiling conditions occur, vanishes at higher injection pressures due to the increase of the spray velocity in the axial direction, as consequence of the momentum growing, became the dominant effect. Finally, Figure 6 reports the effects of the injection pressure on liquid spray penetration under flash boiling conditions. As expected, sprays at higher injection pressures result in a faster spray development. Injection pressures influence the penetration development more significantly for the pressure range between 40.0 and 55.0 MPa. After that, the injection pressure effect on the penetration development diminishes gradually.

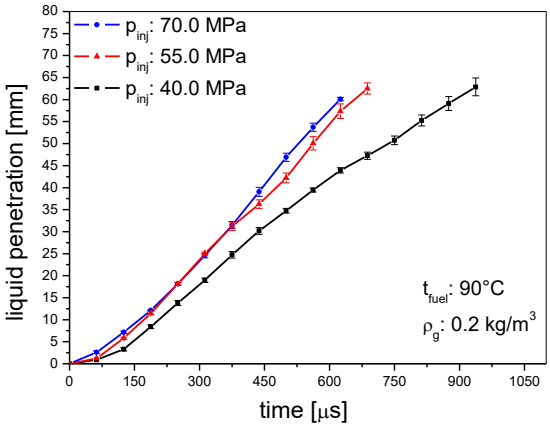

Figure 6. Effect of injection pressure on liquid spray penetration under flash boiling conditions

Conclusions

In this work, a multi-hole GDI injector was used to study mainly the effects of high injection pressure on spray morphology under different ambient and injection conditions. The tests were conducted using commercial gasoline in a heated constant-volume pressurized vessel sprayed through a ten-hole nozzle. The changes in the spray structure and the vaporization processes were investigated over a broad range of ambient conditions by a hybrid optical setup, Z-type shadowgraph and Mie scattering, and using a high-speed C-Mos camera that allowed the acquisition of both the vapor and the liquid phase.

For the experimental conditions considered, the sprays grow in time forming two symmetric lobes including both five jets that fill in uniform way the sampling volume. The results on spray development (quantified in terms of penetration distance) showed a strong function of chamber pressure, and a weaker function of fuel injection pressure. The density of the gas confirmed the braking action on the progress of the fuel resulting the penetrations in an inverse proportionality to the gas densities. Vice versa, just a slight accelerate of the spray was registered with increasing of the injection pressure probably due to the strong fuel atomization that causes a reduction of the droplets size and hence of the spray development. The increase of the ambient temperature generated a strong reduction of the liquid phase along of both the axial and the radial direction because of the vaporization that mainly affects the jets periphery where stronger atomized particles are present. The shadowgraph pictures clearly showed a dense liquid core surrounded by an area including ligaments, finely atomized droplets, and vapor phase. Finally, the investigation under flashing conditions confirmed that the increase of the injection pressure could be considered a way to suppress the spray collapse shape. The accelerate of the spray velocity in the axial direction, due to the increase of the injection pressure, seems to be the dominant element for the spray morphology respect the collapse of the plumes in the central region of the spray induced from flash boiling conditions.

Acknowledgements
The authors would like to acknowledge the Magneti Marelli S.p.A. Powertrain for the hardware supply and the technical support to the experimental work.

Nomenclature

CVC	Constant Volume Vessel
d_0	Hole diameter
DI	Direct Injection
fps:	Frames per second
GDI	Gasoline Direct Injection
L/d	Nozzle length to diameter ratio
LED	Light Emitting Diode
p_a	ambient pressure
p_{inj}	Injection Pressure
PN	Particle Number
ρ_g	Ambient gas density
SI	Spark Ignition
SOI	Start Of Injection
T_{amb}	Ambient temperature
T_{fuel}	Fuel temperature
T_i	Nozzle temperature
t_{inj}	Injector energizing time

References

[1] Hoffmann, G., Befrui, B., Berndorfer, A., Piock, W. et al., "Fuel System Pressure Increase for Enhanced Performance of GDi Multi-Hole Injection Systems," 2014. *SAE Int. J. Engines* 7(1), pp. 519-527.
[2] Klauer N., Klüting M., Schünemann E., Schwarz C., Steinparzer F: "BMW TwinPower Turbo Gasoline Engine Technology - Enabling Compliance with worldwide Exhaust Gas Emissions Requirements," 34th Vienna Motor Symposium, 2013.
[3] Stadler, A., Brunner, R., Härtl, M., Wachtmeister, G., Sauerland, H., "Experimental Investigations on High Pressure Gasoline Injection up to 800 bar for Different Combustion Modes", 27th Aachen Colloquium Automobile and Engine Technology 2018 1089.
[4] Wang, C., Xu, H., Herreros, JM., Wang, J., Cracknell, R., "Impact of fuel and injection system on particle emissions from a GDI engine", 2014, Applied Energy, 132, pp.178-191
[5] Zeng W., Xu M., Zhang Y., Wang Z., "Laser sheet dropsizing of evaporating sprays using simultaneous LIEF/MIE techniques", 2013, Proceedings of the Combustion Institute, 34(1), pp. 1677-1685.
[6] Yang J., Xu M., Hung D.L.S., Wu Q., Dong X., "Influence of swirl ratio on fuel distribution and cyclic variation under flash boiling conditions in a spark ignition direct injection gasoline engine", 2017, Energy Conversion and Management, 138, pp. 565-576.
[7] Dong X., Yang J., Hung D.L.S., Li X., Xu M., "Effects of flash boiling injection on in-cylinder spray, mixing and combustion of a spark-ignition direct-injection engine", 2018, Proceedings of the Combustion Institute,
[8] Senda J., Wada Y., Kawano D., Fujimoto H., "Improvement of combustion and emissions in diesel engines by means of enhanced mixture formation based on flash boiling of mixed fuel", 2008, International Journal of Engine Research, 9(1), pp. 15-27.
[9] Yang J., Dong X., Wu Q., Xu M., "Influence of flash boiling spray on the combustion characteristics of a spark-ignition direct-injection optical engine under cold start", 2018, Combustion and Flame, 188, pp. 66-76
[10] Montanaro, A., Allocca, L., and Lazzaro, M., "Iso-Octane Spray from a GDI Multi-Hole Injector under Non- and Flash Boiling Conditions", 2017, SAE Technical Paper 2017-01-2319.
[11] Hung, D., Harrington, D., Gandhi, A., Markle, L. et al., "Gasoline Fuel Injector Spray Measurement and Characterization - A New SAE J2715 Recommended Practice", 2009, SAE Int. J. Fuels Lubr. 1(1), pp. 534-548.
[12] Allocca, L., Montanaro, A., and Meccariello, G., "Effects of the Ambient Conditions on the Spray Structure and Evaporation of the ECN Spray G," 2019, SAE Technical Paper 2019-01-0283.
[13] Guo H., Ma X., Li Y., Liang S., Wang Z., Xu H., Wang J., "Effect of flash boiling on microscopic and macroscopic spray characteristics in optical GDI engine," 2017, Fuel, 190, pp. 79-89.